

RyR1-mediated moderate endoplasmic reticulum stress is required for myogenic differentiation of myoblasts

Kai Qiu

China Agricultural University

Yubo Wang

China Agricultural University

Doudou Xu

China Agricultural University

Linjuan He

China Agricultural University

Xin Zhang

China Agricultural University

Enfa Yan

China Agricultural University

Jingdong Yin (✉ yinjd@cau.edu.cn)

China Agricultural University <https://orcid.org/0000-0003-4623-0568>

Research Article

Keywords: Ca²⁺ homeostasis, Myogenic induction, RyR1 knockout, Unfolded protein response, Apoptosis, Myoblast

Posted Date: May 10th, 2021

DOI: <https://doi.org/10.21203/rs.3.rs-481993/v1>

License: © ⓘ This work is licensed under a Creative Commons Attribution 4.0 International License.

[Read Full License](#)

Abstract

Background

Cytosolic Ca^{2+} plays vital roles in myogenesis and muscle development. Key mutations of ryanodine receptor 1 (RyR1), a major Ca^{2+} release channel of endoplasmic reticulum (ER), are main causes of severe congenital myopathies. The role of RyR1 in myogenic differentiation has attracted intense research interest, however, it remains unclear.

Methods

This study employed RyR1-knockdown myoblasts and CRISPR/Cas9-based RyR1-knockout myoblasts cells to explore the role of RyR1 in myogenic differentiation, myotube formation as well as the potential mechanism of RyR1-related myopathies.

Results

Cytoplasmic Ca^{2+} concentration was significantly elevated during myogenic differentiation of both primary myogenic cells and myoblasts C2C12 cells, accompanied with a dramatic increase in RyR1 expression and resultant ER stress. Inhibition of RyR1 by siRNA-mediated silence or chemical inhibitor, dantrolene, significantly reduced cytosolic Ca^{2+} , alleviated ER stress, and blocked multinucleated myotube formation. Moderate activation of ER stress effectively relieved myogenic differentiation stagnation induced by RyR1 suppression and demonstrated that RyR1 modulates myogenic differentiation via activation of Ca^{2+} -induced ER stress signaling. RyR1 knockout-induced Ca^{2+} leakage led to severe ER stress and excessive unfolded protein response, and drove cell fate from differentiation into apoptosis.

Conclusions

Therefore, we concluded that dramatic increase in RyR1 expression is required for myogenic differentiation, and RyR1-mediated Ca^{2+} release leading to the activation of ER stress signaling serves a double-edged sword role during myogenic differentiation. This study contributes to a novel understanding of the role of RyR1 in muscle development and related congenital myopathies, and provides a potential target for regulation of muscle regeneration and tissue engineering.

Background

Ryanodine receptor 1 (RyR1), highly expressed in skeletal muscle, is located on the endoplasmic/sarcoplasmic reticulum (ER/SR) membrane. Intracellular flux of Ca^{2+} mediated by RyR1 is required for skeletal muscle contraction. Various mutations or epigenetic changes in the RyR1 gene have been associated with muscle myopathies mainly including malignant hyperthermia and several congenital myopathies [1–4]. Diagnostic gene-sequencing has been employed to avoid RyR1-related

congenital myopathies. Several disease-modulating therapeutic strategies and salvage therapies have also been developed against RyR1-related myopathies [5–9].

RyR1 attracts intense interest in the field of medicine because it is a Ca^{2+} channel of great clinical significance. The crystal structure of RyR1 has been determined by electron cryomicroscopy to be a 6-transmembrane ion channel with an EF-hand domain for Ca^{2+} -mediated allosteric gating and a huge cytoplasmic domain on top of each transmembrane domain [10–12]. Ca^{2+} signaling is important for myogenic gene expression and skeletal muscle differentiation [13]. RyRs-mediated Ca^{2+} release plays a role in the histogenesis of mammalian skeletal muscle, and the block of RyRs selectively inhibits fetal myoblast differentiation [14]. Mutations in RyR1 that results in leaking of the internal Ca^{2+} store can have both physiological and pathological consequences [15].

A naturally occurring single-base mutation of RyR1 closely was associated with malignant hyperthermia of pigs but has been particularly enriched in genetic selections for muscle growth rate and lean body mass [16]. Homozygous RyR1-null mice died after birth and displayed small limbs and abnormal skeletal muscle organization [17, 18]. Presumably, RyR1 is not only associated with myopathies, but is implicated in myogenesis and subsequent muscle development. However, the mechanisms of RyR1 action in myogenesis have not been elucidated.

Alterations in cellular Ca^{2+} dynamics directly trigger ER stress and activate the unfolded protein response (UPR) [19, 20]. ER/SR is a membrane-bound organelle in mammalian cells that is responsible for proper folding, processing, and trafficking of proteins and also plays an important role in cellular Ca^{2+} homeostasis. ER stress and UPR modulation are implicated in various human diseases including sarcopenia [21–23]. In recent decades, roles of ER stress and UPR pathways in skeletal muscle health and disease have received increased research attention [24]. In addition to induction of apoptosis, ER stress positively influences myogenic differentiation and myofiber formation [25, 26]. Therefore, we surmise that ER stress signaling is involved in RyR1-mediated muscle development.

Satellite cells and myoblasts play a pivotal role in the repair and maintenance of skeletal muscle by differentiating into mature myocytes [27]. In this study, we hypothesized that RyR1-mediated Ca^{2+} dynamics delicately balance ER stress-induced apoptosis and myoblast differentiation. To test this theory, we employed RyR1-KO myoblasts established by CRISPR/Cas9 gene-editing and RyR1-weaken cells to explore the role of RyR1 in myogenic differentiation and formation mechanism of RyR1-related myopathies.

Materials And Methods

Cell culture and myogenic differentiation

Mouse skeletal myoblast C2C12 cells were purchased from the National Infrastructure of Cell Line Resource in China. Proliferating myoblasts were maintained in DMEM/high glucose medium (Hyclone,

Logan, UT, USA) supplemented with 10% FBS (Gibco, Carlsbad, CA, USA) in a humidified CO₂ incubator (5% CO₂, 37 °C; HF90, Heal Force, Hongkong, China). For myogenic differentiation, myoblasts with 80%~90% confluence were induced by DMEM/high glucose medium supplemented with 2% horse serum (Hyclone, Logan, UT, USA).

Myogenic cells of pigs (n = 3) were isolated using preplate techniques from skeletal muscle according to our previous reports [28]. The cells were cultured in growth medium in a dish coated with collagen I (Sigma-Aldrich) at 37 °C and 5% CO₂. The growth medium was composed of DMEM/F12 (Hyclone), 10% FBS (Gibco-BRL, Carlsbad, CA, USA), 2 mM glutamine (Gibco-BRL), and 5 ng/mL bFGF (Peptech, Burlington, MA, USA). As for myogenic induction, cells were cultured for 5 days in DMEM/F12 medium containing 2% horse serum (Hyclone).

Cellular Ca²⁺ concentration measurement

Ca²⁺ concentration in the cytoplasm or ER was measured using flow cytometry. Cells were collected, washed three times with PBS and HBS respectively, and then incubated in 5µg/mL Fluo-3 acetoxymethyl ester (Cayman, Ann Arbor, MI, USA) or Mag-fluo-AM (GENMED, Shanghai, China) for 30 min at 37 °C in dark. After three washes with PBS supplemented with 1% FBS, cells were resuspended in 200 µL PBS containing 1% FBS. Flow cytometry was carried out immediately using a FACS Calibur Cytometer and Image Cytometry software (BD, Franklin, NJ, USA). Calcium-bound Fluo-3 or Mag-fluo-AM has an emission maximum of 526 nm which was quantified by excitation with a 488-nm laser and signals were collected using a 530/30 nm band-pass filter. Each sample generated 20,000 live gated events. Debris, multicellularity, and dead cells were excluded by forward scatter (FSC) and side scatter. For detecting dynamic change of Ca²⁺ concentration of cells during myogenic differentiation, a blank control combined with a house-keeping control (the proliferative C2C12 cells) was used to correct the deviation caused by the loaded indicator amount and the voltage used in each measurement. Mean fluorescence intensity was determined from the entire cell population and then adjusted by relative cell size calculated according to FSC to represent Ca²⁺ concentration.

Cell viability and apoptosis assays

Cell vitality was detected using Cell Counting Kit-8 (CA1210, Solarbio, Beijing, China). According to the experimental protocol, cells were cultured in 96-well plates for 24 h, and then CCK-8 reagent was added at 100 uL per well. One hour later, the absorbance of culture medium was analyzed by microplate spectrophotometer. In addition, cell proliferation activity was also measured by Cell-Light™ EdU Apollo@488 Cell Tracking Kit (RIBOBIO, Guangzhou, China). After pre-cultured for 24 h in 96-well plates, cells were cultured continuously for another 2 h in new media supplemented with 50 µmol/L EdU reagent. Then cells were fixed by 4% paraformaldehyde, permeabilized by 0.2% Triton X-100, and fluorescently-tagged with Hoechst33342 using nucleus staining methods. The newly proliferated cells were visualized by an Apollo reaction system. Cell proliferation rate was analyzed by ImageJ (v1.51h, National Institutes of Health, Bethesda, MD, USA).

Apoptosis was detected using an Annexin V-FITC/PI Apoptosis Detection Kit (Gene Protein Link, Beijing, China) according to the manufacturer's protocol. Briefly, cells were stained with a combination of Annexin V-FITC and propidium iodide in darkness for 15 min at room temperature, and then analyzed by the flow cytometry system.

RNA isolation and qRT-PCR

Cells used for total RNA extraction obtained from 3 separate experiments (different batches of cells and on different days). Total RNA was extracted from cells using HiPure Total RNA Mini Kit (Magen, Beijing, China), and then reverse-transcribed into cDNA using a PrimeScript™ RT reagent Kit with gDNA Eraser (Takara, Osaka, Japan). Synthesized cDNA was used for RT-qPCR analysis by employing a quantitative real-time PCR kit (Takara, Osaka, Japan) with an AJ qTOWER 2.2 Real-Time PCR system (Analytik Jena AG, Jena, Germany) according to standard procedures. All samples were measured in triplicate. The primers used in the experiment were listed in **Additional file 4: Table S1**. For the comparison of RyR1 and RyR3 expression in cells, the amplification efficiency of their primers was used firstly to rectify the qRT-PCR cycle number. GAPDH was used as an internal control. Relative gene expression level was calculated by $2^{-\Delta\Delta Ct}$ method.

Protein extraction and western blot analysis

The relative abundances of proteins related to ER stress, MAPK signaling pathway, and apoptosis were determined by Western Blot. Cell samples were collected and lysed in RIPA buffer (Huaxingbio, Beijing, China) composed of 50 mM Tris-HCl (pH 7.4), 150 mM NaCl, 1% NP-40, and 0.1% SDS, plus a Halt protease/phosphatase inhibitor cocktail (Thermo Fisher Scientific, Waltham, MA, USA). The homogenate was centrifuged at $14,000 \times g$ for 15 min at 4°C and the supernatant was isolated for Western Blot analysis. Protein concentrations were determined using a BCA Protein Assay Kit (Huaxingbio, Beijing, China). Equal amounts of protein (30 µg), together with a pre-stained protein ladder (Thermo Fisher Scientific, Waltham, MA, USA), were electrophoresed on SDS polyacrylamide gel, electro-transferred to a polyvinylidene difluoride membrane (Millipore, Bedford, OH, USA), and blocked for 1 h in 5% non-fat dry milk at room temperature in Tris-Buffered saline and Tween-20 (TBST; 20 mmol/L Tris-Cl, 150 mmol/L NaCl, 0.05 % Tween 20, pH 7.4). Samples were incubated with corresponding primary antibodies overnight at 4°C. After washing with TBST (pH 7.4), membranes were incubated with the secondary antibody (DyLight 800, Goat Anti-Rabbit IgG). Protein bands were detected with the Odyssey Clx kit (LI-COR, Lincoln, NE, USA) and quantified using an Alpha Imager 2200 (Alpha InnoTec, CA, USA). Relative protein expression was calculated by taking GAPDH as an internal standard. Information of antibodies used for Western Blot in this study was listed in **Additional file 5: Table S2**.

Immunocytochemistry

Cells were fixed with 4% paraformaldehyde (PFA)/PBS for 30 min. After the neutralization of excess formyl group by 2 mg/mL glycine, cells were permeabilized by 0.2% Triton X-100 in PBS for 10 min. After blocked with 3% BSA/PBS, cells were incubated with primary antibody (anti-RyR1, 1:300, MA3-925,

Thermo Fisher Scientific, Waltham, MA, IL, USA; anti-myosin, 1:300, M4276, Sigma-Aldrich, Louis, MO, USA) overnight and then incubated with Fluorescein-Conjugated secondary antibody (ZF-0311, ZSGB-BIO, Beijing, China) at 1:100. Nuclei were stained with DAPI (Thermo Fisher Scientific, Waltham, MA, USA). Finally, myotubes were visualized by an inverted fluorescence microscope.

Chemical blockers of Ca²⁺ channels

Two kinds of chemical blocker were used for the experimental treatments. DAN (Stock solution: 200 mM in DMSO, HY-12542A, MedChemExpress, South Brunswick, NJ, USA) was added as a final concentration of 10 μ M in culture media. THA (ab120286), purchased from Abcam (Cambridge, UK), was used at a final concentration of 100 nM in culture media. Equal amounts of vehicle (DMSO) were used as the control. During the proliferating period, myoblasts were treated with chemical blocker for 48 h and then collected for further analysis. Upon myogenic induction, myoblasts were treated with chemical blocker for 5 days and then used for mRNA extraction and immunocytochemistry. Each treatment was conducted in three independently repeated experiments.

Small interfering RNA transfection

RNA interference of RyR1 (mouse, gene ID: 20190) was performed using a 21-base pair small interfering RNA (siRNA) duplex (designed and synthesized by IBSBIO, Shanghai, China). The sense strand nucleotide sequence for RyR1 siRNA was 5'-CCUGCUCUAUGAACUUCUAGC-3' (sense strand) and 5'-UAGAAGUUCAUAGAGCAGGUU-3' (anti-sense strand). A scrambled siRNA (siControl, sense strand: 5'-UUCUCCGAACGUGUCACGUTT-3', anti-sense strand: 5'-ACGUGACACGUUCGGAGAATT-3') with the same nucleotide composition as RyR1 siRNA but lacks significant sequence homology to the RyR1 was also designed as a negative control. Briefly, myoblasts were plated in a cell culture dish for 24 h, and then transfected using Lipofectamine 3000 (Invitrogen, Carlsbad, CA, USA) according to the manufacturer's protocol with 100 nM siRNA. After transfection for 24 h, myogenic differentiation was induced in cells.

CRISPR/Cas9 gene-editing

Gene-edited myoblasts with RyR1-knockout were generated via the Clustered Regularly Interspaced Short Palindromic Repeats (CRISPR)-CRISPR associated protein 9 (Cas9) system. The plasmid vectors expressing Cas9 protein and guide-RNA (gRNA) were designed and synthesized by Syngentech (Beijing, China). One gRNA among the three gRNA targeting RyR1 was selected for using in further study according to their shearing efficiency. The sequences of gRNA-1, gRNA-2, and gRNA-3 are as follows: 5'-GGCGATGATCTCTATTCTTA-3', 5'-TACAGCCCCTACCCCGGAGG-3', and 5'-AGCTCAGGCCACCCACCTGA-3', respectively. The transient transfection of CRISPR-Cas9 vectors was achieved by electroporation using Nucleofector Program B-032 (VCA-1003, Lonza, Basel, Switzerland). Infected myoblasts were selected by incubation with 200 μ g/mL hygromycin for 1 week. The stable RyR1-knockout cell line was obtained through single cell clone techniques. Genotype identification and verification of putative off-target sites (**Additional file 6: Table S3**) were conducted via DNA-sequencing technology. The related primers were list in **Additional file 7: Table S4**.

Statistical analysis

Data were analyzed using t-test procedures of SAS software (Version 9.3, SAS Institute, Cary, NC, USA) and presented as mean \pm S.E.M. The criterion for statistical significance was set at $P < 0.05$.

Results

Cytoplasmic Ca^{2+} dynamics and expression patterns of Ca^{2+} channels during myogenic differentiation

Upon myogenic induction, myoblasts gradually expressed plenty of myosin from the day 0 to 6 (**Additional file 1: Figure S1A**) and protein expression of RyR1 was significantly increased at day 6 (**Additional file 1: Figure S1B, C**). During the entire period (day 1-5) of myogenic differentiation, cytoplasmic Ca^{2+} concentration (labeled by Fluo-3) of myoblasts was significantly increased (**Additional file 1: Figure S1D, E**).

Myf5 (myogenic factor 5) and *MyoD1* (myogenic differentiation 1) expression were significantly increased on day 2 relative to day 0, then sharply decreased on day 6 and 8 and even lower than the initial level during myogenic induction (**Figure 1A, B**). *MyoG* (myogenin) expression showed continuous increase and reached a plateau on day 4 (**Figure 1C**).

As for Ca^{2+} transporters, CAV1.1 (also known as CACNA1S, calcium voltage-gated channel subunit alpha1 S), CRACR2B (calcium release activated channel regulator 2B), ITPR1 (inositol 1,4,5-trisphosphate receptor type 1), and ORAI2 (ORAI calcium release-activated calcium modulator 2) showed similar expression pattern with *Myf5* and *MyoD1* (**Figure 1D-G**). The expression patterns of RyR1 and STIM1 (stromal interaction molecule 1) matched *MyoG* expression pattern well. Notably, RyR1 mRNA expression showed greater 100-fold increase (**Figure 1H, I**), while RyR3 mRNA expression was less than 1/10 of RyR1 in C2C12 cells, and the increase in RyR3 mRNA expression was far below that of RyR1 during myogenic differentiation (**Additional file 2: Figure S2A, B**), therefore, the major role of RyRs involved in myogenesis of C2C12 cells can be attributed to RyR1. Consistently, RyR1 mRNA expression showed almost a 25-fold increase during myogenic differentiation, while the mRNA expression of RyR3 was not changed in myogenic cells derived from pigs (**Additional file 2: Figure S2C-E**). In addition, the mRNA expression of ATP2A2 (ATPase ER/SR Ca^{2+} transporting 2; **Figure 1J**), ATP2B (ATPase plasma membrane Ca^{2+} transporting 1; **Figure 1K**), and CRACR2A (calcium release activated channel regulator 2A; **Figure 1L**) was significantly increased on day 2 and maintained a plateau on day 2-8 during myogenic induction of C2C12 cells.

As shown in **Figure 2A, B**, cytoplasmic Ca^{2+} concentration was significantly decreased by treatment with dantrolene (DAN), an inhibitor of RyR1, which blocks the release of Ca^{2+} from SR/ER [29]. RyR1 knockdown by siRNA significantly decreased cytoplasmic Ca^{2+} concentration of C2C12 cells (**Figure 2C, D**). The protein expression of RyR1 was effectively suppressed by siRNA interference (**Figure 2E, F**). Functional constraints of RyR1 realized by either DAN or siRyR1 dramatically inhibited the formation of

multinucleated myotubes of myoblasts (**Figure 2G, H**). Upon myogenic induction, DAN effectively blocked *MyoD1* expression on day 2 and both *MyoG* and *Mymk* (myomaker, myoblast fusion factor) expression on day 4 (**Figure 2I**). At the day 4 during myogenic induction, siRyR1-knockdown significantly reduced RyR1, *MyoG*, and *Mymk* expression without effects on *Myf5* and *MyoD1* expression (**Figure 2J**).

RyR1-induced ER stress is indispensable for myogenic differentiation

During myogenic differentiation of C2C12 myoblasts, the mRNA expression of protein disulfide isomerases including ERP44 (ER protein 44), PDIA3 (protein disulfide isomerase associated 3), and PDIA4 (protein disulfide isomerase associated 4) which are present in ER, was significantly increased relative to those before differentiation (**Figure 3A**). Endoplasmic membrane proteins ATF6 (activating transcription factor 6) and EIF2AK3 (eukaryotic translation initiation factor 2 alpha kinase 3), considered as typical ER stress markers, also showed significantly higher mRNA expression (**Figure 3B**). Furthermore, the mRNA expression of apoptosis- and heat stress- related proteins including BAX (BCL2-associated X protein), caspase-12, DDIT3 (DNA-damage inducible transcript 3), HSP90B1 (heat shock protein 90, beta, member 1), and HSPA5 (heat shock protein 5) was also significantly stimulated during myogenic differentiation (**Figure 3C**). Similarly, significantly increased mRNA expression of protein disulfide isomerases, ERP44 and PDIA3, were also observed in primary myogenic cells derived from skeletal muscle of pigs during myogenic differentiation relative to those before differentiation (**Figure 3D**). Simultaneously, mRNA expression of ER stress markers, ATF6 and EIF2AK3, increased significantly (**Figure 3E**). The mRNA expression of apoptosis- and heat stress- related proteins including caspase-9, DDIT3, and HSPA5 was also significantly stimulated (**Figure 3F**). The phosphorylation of IRE1 α and PERK was significantly reduced by DAN treatment compared with the control, while EIF2 α was not altered (**Figure 3G, H**). For MAPK signaling (**Figure 3I, J**), phosphorylation level of Erk1/2 (extracellular regulated protein kinases) was significantly increased by DAN treatment, while JNK (stress-activated protein kinase/Jun-amino-terminal kinase) was decreased.

THA treatment significantly increased cytoplasmic Ca²⁺ concentration (**Figure 4A, B**), but did not influence the mRNA expressions of myogenic-specific genes including *Myf5*, *MyoD1*, *MyoG* and *Mymk* (**Figure 4C**). RyR1-knockdown realized by siRNA interference was independent on THA treatment (**Figure 4D, E**). As shown in **Figure 3F, G**, on day 4 during myogenic induction, RyR1-silencing significantly decreased phosphorylation of IRE1 α , PERK, and EIF2 α . Meanwhile, THA did not influence IRE1 α and EIF2 α phosphorylation, but tended to increase PERK phosphorylation in myoblasts. Obviously, THA recovered the decreased phosphorylation level of IRE1 α , PERK, and EIF2 α caused by siRyR1-knockdown.

On day 4 during myogenic induction, siRyR1-knockdown significantly increased *Myf5* and *MyoD1* mRNA expression but decreased *MyoG* and *Mymk* expression. Alterations in *Myf5*, *MyoD1*, *MyoG* and *Mymk* mRNA expressions caused by siRyR1-knockdown were effectively eliminated by THA treatment. In addition, mRNA expression of *Myf5*, *MyoD1*, *MyoG* and *Mymk* was not influenced by THA in myoblasts with absence of siRyR1-knockdown (**Figure 5A**). Accordingly, THA treatment did not affect myogenic

differentiation of myoblasts with absence of siRyR1-knockdown. In particular, myotube formation was significantly inhibited by siRyR1-knockdown, which was effectively recovered by THA (**Figure 5B, C**).

Effects of RyR1-knockout on cell proliferation and differentiation

As shown in **Additional file 3: Figure S3**, the frame-shift mutation of RyR1 was realized by the CRISPR/Cas-9 gene editing system targeting Exon 18 of RyR1 via gRNA-3, which showed the highest shearing efficiency among three designed gRNA. Homozygote and heterozygote of RyR1-knockout cells, named as RyR1^{-/-} and RyR1^{+/-}, were obtained by monoclonal cultivation and identified via gene sequencing on the target site and putative off-target sites of gRNA-3. Relative to the wild type cells (WT), RyR1^{-/-} showed higher Ca²⁺ concentration in cytoplasm, but lower Ca²⁺ level in the ER (**Figure 6A-C**). The mRNA expression of ATP2A2, ATP2B, CRACR2B, and ORAI1 was significantly increased, while CAV1.1 and ORAI2 expression were decreased in RyR1^{-/-} or RyR1^{+/-} relative to WT (**Figure 6D**).

Cell proliferation viability (the proportion of EdU⁺ cells) of RyR1^{-/-} or RyR1^{+/-} significantly declined relative to WT (**Figure 6E, F**), which was also demonstrated by the CCK-8 test (**Figure 6G**). As shown in **Figure 6H**, the mRNA expression of *Myf5*, *MyoD1*, and *MyoG* was significantly increased in RyR1^{-/-} or RyR1^{+/-} relative to WT. RyR1-knockout significantly reduced phosphorylation of Erk1/2 and JNK, as well as the total protein of JNK (**Figure 6I, J**).

Apoptosis triggered by RyR1-knockout

On day 2 during myogenic induction, apoptosis instead of myotube formation was accelerated in both RyR1^{-/-} and RyR1^{+/-}. The apoptosis rate of RyR1^{-/-} and RyR1^{+/-} was significantly increased relative to WT (**Figure 7A, B**). The protein level of cyclin D1 and caspase-3 was significantly lower in RyR1^{-/-} or RyR1^{+/-}, but the expression of cleaved caspase-3 was significantly increased as compared with WT (**Figure 7C, D**).

ER stress level in RyR1^{-/-} and RyR1^{+/-} was evaluated by Western Blot (**Figure 7E**). Both phosphorylated and total protein expression of IRE1 α and PERK were dramatically elevated by RyR1-knockout, while phosphorylation of EIF2 α was significantly decreased (**Figure 7F**). As to several apoptosis-related proteins, the protein abundance of CHOP (also known as DDIT3), caspase-9, and caspase-12 in RyR1^{-/-} or RyR1^{+/-} was significantly increased relative to WT, while the expression of ERP44 and HSPA5 was not influenced (**Figure 7G, H**).

Discussion

Skeletal muscle mass is maintained by myogenic differentiation of myogenic progenitors [30], in which cytosolic Ca²⁺ regulation plays a vital role [28]. Myotube formation requires net Ca²⁺ influx into myoblasts [31-33]. RyR1, serving as a major Ca²⁺ release channel of ER, has attracted the most intense research interest among intracellular Ca²⁺ channels. However, the role of RyR1 in myogenic differentiation remains unclear.

RyR1 protein expresses during differentiation in C2C12 cells which provides an appropriate model for investigations of RyR1 function during myogenic differentiation [34]. In the current study, we observed that cytoplasmic Ca^{2+} concentration of C2C12 myoblasts was significantly elevated during myogenic differentiation. K Qiu, D Xu, L Wang, X Zhang, N Jiao, L Gong, et al. [28] also observed increased Ca^{2+} concentration in primary myogenic cells of pigs. Cellular Ca^{2+} is tightly regulated by channels and transports [35]. Relative to the extracellular matrix and ER, cytoplasmic Ca^{2+} concentration is maintained at very low levels (10-100 nM) under resting conditions. Ca^{2+} is released from the ER, the main storage site of intracellular Ca^{2+} , through the transmembrane channels RyR1 and ITPR1 [36, 37]. Cytoplasmic Ca^{2+} influx from extracellular matrix occurs through plasma membrane channels, CAV1, CAV2, and CAV3 [38]. To maintain the resting state, excessive amounts of cytoplasmic Ca^{2+} re-accumulates in the ER by SR/ER Ca^{2+} -ATPase (SERCA, also called ATP2A) [39] or is expelled in the external milieu by plasma membrane Ca^{2+} -ATPase (PMCA, also called ATP2B) [40, 41]. Furthermore, store-operated calcium entry (SOCE), mediated by STIM (ER Ca^{2+} sensors), activates CRAC and ORAI channels located at plasma membrane to maintain cellular Ca^{2+} homeostasis [42, 43].

Lineage commitment and differentiation of myoblasts are governed by the programmed expression and functional activation of myogenic regulatory transcription factors (*MRFs*) [44, 45]. In this study, we clearly demonstrated the expression pattern of Ca^{2+} transporters as well as *MRFs* during myogenic differentiation and especially discovered RyR1 expression was increased more than 100-fold in C2C12 cells and almost 25-fold in myogenic cells of pigs during myogenic differentiation. CAV1.1 is a physiological activator of RyR1 in the excitation–contraction coupling of skeletal muscle [46]. In this study, the expression of CAV1.1 was not significantly increased as RyR1 during myogenic differentiation, which indicated that RyR1 expression in myogenic cells is not activated by the expression of CAV1.1 but probably induced by the surroundings, such as myogenic medium and cellular density. Notably, RyR1 restriction via either DAN treatment or siRNA interference significantly decreased cytoplasmic Ca^{2+} concentration, and then blocked formation of multi-nuclei myotubes and expression of *MRFs*. As a major Ca^{2+} release channel of ER, the dramatic increase of RyR1 expression should be responsible for the significant elevation of cytosolic Ca^{2+} concentration. Therefore, we deduced that dramatic increase of RyR1 expression is required for myogenic differentiation.

Alterations in Ca^{2+} dynamics can trigger ER stress and activation of the UPR [19, 20]. In the current study, expressions of protein disulfide isomerases in the ER including ERP44, PDIA3, and PDIA4, directly reflecting the oxidation state of ER [47], and were significantly increased during myogenic differentiation. Moreover, we observed that ER transmembrane proteins including protein kinase RNA-like ER kinase (PERK/EIF2AK3) and activating transcription factor 6 (ATF6), involved in the UPR process as sensors [48], were elevated upon myogenic induction. Therefore, ER stress signaling was activated by the dramatic increase of RyR1 expression in myoblasts during myotube formation.

IRE1 α , PERK and ATF6 function as UPR stress sensors. UPR transmits information about the protein-folding status in the ER lumen to the nucleus and cytosol, and buffers fluctuations in unfolded protein load via UPR stress sensors. Upon activation of ER stress, PERK phosphorylates initiation factor eukaryotic translation initiator factor 2 α (eIF2 α) and attenuates general protein synthesis [48]. ATF6-transmitted ER stress signaling results in apoptosis during muscle development [26]. ER stress is always accompanied by activation of a series of stress-induced protein phosphorylation involved in the MAPK signaling pathways. For example, JNK protein kinases can be activated by the coupling of ER stress and transmembrane protein kinase IRE1 [49]. In addition, the activation of the Erk1/2 pathway is important for cells to avoid apoptosis caused by physical stress [50]. In our study, inhibition of RyR1 function by DAN treatment significantly reduced phosphorylation levels of IRE1 α , PERK, and JNK proteins, but obviously increased Erk1/2 phosphorylation, demonstrating that DAN-induced RyR1 function restriction effectively and specifically alleviated ER stress.

Thapsigargin (THA), a well-characterized ER stress-inducing agent, was used to trigger ER stress through inhibiting microsomal Ca²⁺-ATPase, disrupting cellular Ca²⁺ homeostasis, and accumulating unfolded proteins in the ER lumen [51]. In the current study, the dose of THA was far below that used in previous studies [52, 53] to gain a moderate ER stress status, and guaranteed that THA did not influence the efficiency of siRyR1-knockdown. As a result, THA treatment did not trigger severe ER stress compared with the control. Furthermore, THA treatment significantly increased cytoplasmic Ca²⁺ concentration but did not affect expression of myogenic specific genes. We observed that ER stress alleviated by RyR1 suppression was dramatically intensified by THA addition. At the same time, myotube formation inhibited by siRyR1-knockdown was also recovered by THA treatment, accompanied by the expression of *MRFs*. Therefore, RyR1-mediated ER stress was indispensable for myogenic differentiation.

C/EBP homologous protein (CHOP) encoded by DDIT3 gene is a member of the CCAAT/enhancer-binding protein (C/EBP) family of transcription factor, whose expression is stimulated during ER stress [54]. Caspase-12 is specifically activated during ER stress-mediated apoptosis especially caused by the disruption of ER Ca²⁺ dynamic [55]. Caspase-9 activates apoptotic signals when mitochondria are damaged [56]. The localization of BAX from cytoplasm to mitochondria is a necessary process of apoptosis [57]. The HSPA5 gene encodes the binding immunoglobulin protein (BiP), a member of the heat shock protein 70 (HSP70) family localized in the ER lumen. Once ER stress overwhelms, BiP can initiate the UPR and decrease unfolded/misfolded protein load of the ER to assist cell survival by avoiding the activation of apoptosis machinery [58, 59]. HSP90B1 (also called GRP94 or gp96), located in the ER, plays important roles in stabilizing and folding other proteins [60]. ERP44, a ER folding assistant of the thioredoxin family, is induced during ER stress for protein quality control [61]. In our study, myogenic induction not only increased expression of proteins related to ER stress-induced apoptosis, including DDIT3, caspase-12, and BAX, but also enhanced expression of proteins that mitigate ER stress, such as ERP44, HSP90B1, and HSPA5. Under the pressure of ER stress-induced apoptosis, cells express high levels of heat stress proteins (HSPA12A, HSP90B1, HSPA4, HSPA5 and HSPA6) to increase their adaptability [62]. Therefore, we deduced that a certain degree of ER stress-induced apoptosis was

triggered during myogenic differentiation but balanced by the enhanced protection mechanism against ER stress per se.

To further explore the roles of RyR1 in myogenic differentiation and muscle development, a model of RyR1-KO myoblasts established by CRISPR/Cas9 gene-editing was employed in this study. RyR1 Ca^{2+} release channels are composed of macromolecular complexes consisting of a homotetramer of 560-kDa RyR1 subunits that form scaffolds for proteins that regulate channel function including protein kinase A (PKA) and the phosphodiesterase PDE4D3 (both of which are targeted to the channel via the anchoring protein mAKAP), PP1 (targeted via spinophilin), and calstabin1 (FKBP12) [63, 64]. The deletion of RyR1 probably resulted in the dysfunction of the protein complex, losing the control of Ca^{2+} flowing out of the ER and accelerated Ca^{2+} flooding into the cytoplasm from the ER, which also distorted the expression patterns of other Ca^{2+} transporters. This observation is consistent with previous studies that demonstrated both over-activation and mutations of RyR1 resulted in leakage of Ca^{2+} from the SR [9, 65]. Cytoplasmic Ca^{2+} elevation directly activated ER stress [19, 20], and has a strong influence on differentiation through oxidative signaling and G0/G1 cell cycle arrest [66]. In the current study, expression of Cyclin D1 was abolished and viability of RyR1-KO cells was decreased, demonstrating that cell cycle and metabolism was suppressed by the enhanced ER stress caused by RyR1-KO mediated cytoplasmic Ca^{2+} elevation.

ER stress signaling can give rise to myogenic differentiation and apoptosis [25]. In the present study, differentiation potential of RyR1-KO myoblasts reflected by *MRFs* expression was dramatically enhanced. However, the differentiation process of RyR1-KO myoblasts was interrupted by programmed cell death through apoptosis during myogenic induction, which indicated that RyR1 knockout reduced the capacity of cells to adapt to the surroundings, such as the differentiation medium containing 2% horse serum. UPR was a protective response for cells under stress, while excessive or prolonged UPR can cause apoptosis [67]. Caspase-3, belonging to a highly conserved family of cysteinyl aspartate-specific proteases, is an essential regulator of apoptosis. In the current study, cleaved activation of caspase-3 in RyR1-KO cells was significantly stimulated, which is supported by a previous study of RyRs-mediated ER stress [68]. The total and phosphorylated protein expressions of IRE1 α and PERK were sharply increased in RyR1-KO cells, indicating that RyR1 deletion activated serious ER stress through ER Ca^{2+} leakage. Furthermore, aggravated ER stress significantly increased expression of CHOP, caspase-9, and caspase-12. Nonetheless, the positive effects of ERP44 and HSPA5 against ER stress were not enhanced in RyR1-KO myoblasts. In addition, phosphorylation levels of JNK and Erk1/2, whose activations are beneficial for the resistance to ER stress-induced apoptosis [49, 50], were also significantly reduced in RyR1-KO cells. Therefore, we deduced that RyR1 deletion led to more serious ER stress and excessive UPR than the tolerance thresholds of cells, and accounted for the apoptosis of RyR1-KO myoblasts upon myogenic induction.

Conclusions

In summary, dramatically increased RyR1 expression which activated ER stress signaling through increased cytoplasmic Ca^{2+} was absolutely indispensable for myogenic differentiation. We discovered a novel role of RyR1 acting as a double-edged sword in myogenic differentiation by swaying the fate of myoblasts between differentiation and apoptosis. Our study contributes to the knowledge of the role of RyR1 in myogenic differentiation and related congenital myopathies, and provides a potential target to regulate muscle regeneration and related tissue engineering.

Abbreviations

ATF6	Activating transcription factor 6
ATP2A2	ATPase ER/SR Ca ²⁺ transporting 2
ATP2B	ATPase plasma membrane Ca ²⁺ transporting 1
BAX	BCL2-associated X protein
BiP	Binding immunoglobulin protein
C/EBP	CCAAT/enhancer-binding protein
Cas9	CRISPR associated protein 9
CASP3	Caspase-3
CAV1.1	Calcium voltage-gated channel subunit alpha1 S
CHOP	C/EBP homologous protein
CRACR2A	Calcium release activated channel regulator 2A
CRACR2B	Calcium release activated channel regulator 2B
CRISPR	Clustered Regularly Interspaced Short Palindromic Repeats
DAN	Dantrolene
DDIT3	DNA-damage inducible transcript 3
EIF2AK3	Eukaryotic translation initiation factor 2 alpha kinase 3
eIF2 α	Eukaryotic translation initiation factor 2 α
ER	Endoplasmic reticulum
Erk1/2	Extracellular regulated protein kinases
ERP44	ER protein 44
FKBP12	Calstabin1
FSC	Forward scatter
gRNA	Guide-RNA
HSP70	Heat shock protein 70
HSP90B1	Heat shock protein 90, beta, member 1
HSPA5	Heat shock protein 5
ITPR1	Inositol 1,4,5-trisphosphate receptor type 1
JNK	Stress-activated protein kinase/Jun-amino-terminal kinase
MRFs	Myogenic regulatory transcription factors
Myf5	Myogenic factor 5
Mymk	Myomaker
MyoD1	Myogenic differentiation 1
MyoG	Myogenin

ORAI2	ORAI calcium release-activated calcium modulator 2
OTS	Off-target sites
PDIA3	Protein disulfide isomerase associated 3
PDIA4	Protein disulfide isomerase associated 4
PERK/EIF2AK3	Protein kinase RNA-like ER kinase
PKA	Protein kinase A
RyR1	Ryanodine receptor 1
SOCE	Store-operated calcium entry
SR	Sarcoplasmic reticulum
STIM1	Stromal interaction molecule 1
TBST	Tris-Buffered saline and Tween-20
THA	Thapsigargin
UPR	Unfolded protein response
WT	Wild type

Declarations

Acknowledgements

Not applicable.

Authors' contributions

JY obtained financial support and oversaw the study; JY and KQ conceptualized this study, analyzed and interpreted the data, and drafted the manuscript; KQ, YW, DX, LH, XZ, and EY performed the experiments. All authors contributed, commented, and approved the final content of the manuscript.

Funding

This study was financially supported by the National Natural Science Foundation of China (Grant No. 31790412), National key research and development program of China (Grant No. 2018YFD0500402), and the National Natural Science Foundation of China (Grant No. 31672431).

Availability of data and materials

All data generated or analyzed during this study are included in this published article and its supplementary information files.

Declarations

Ethics approval and consent to participate

All studies using pigs were conducted in accordance with the guidelines of, and approved by, the Institutional Animal Care and Use Committee of China Agricultural University.

Consent for publication

Not applicable.

Competing interests

The authors declare no conflict of interest.

References

1. Ravenscroft G, Davis MR, Lamont P, Forrest A, Laing NG. New era in genetics of early-onset muscle disease: Breakthroughs and challenges. *Semin Cell Dev Biol.* 2017; 64:160-170. doi: 10.1016/j.semcdb.2016.08.002.
2. Rokach O, Sekulic-Jablanovic M, Voermans N, Wilmshurst J, Pillay K, Heytens L, et al. Epigenetic changes as a common trigger of muscle weakness in congenital myopathies. *Hum Mol Genet.* 2015; 24(16):4636-4647. doi: 10.1093/hmg/ddv195.
3. Maclennan DH, Duff C, Zorzato F, Fujii J, Phillips M, Korneluk RG, et al. Ryanodine receptor gene is a candidate for predisposition to malignant hyperthermia. *Nature.* 1990; 343(6258):559-561. doi: 10.1038/343559a0.
4. Rachel R, Danielle C, Marie-Anne S, Jane H, Philip H. Mutations in RYR1 in malignant hyperthermia and central core disease. *Hum Mutat.* 2006; 27(10):977-989. doi: 10.1002/humu.20356.
5. Lawal TA, Todd JJ, Meilleur KG. Ryanodine Receptor 1-Related Myopathies: Diagnostic and Therapeutic Approaches. *Neurotherapeutics.* 2018; 15(4):885-899. doi: 10.1007/s13311-018-00677-1.
6. Suman M, Sharpe JA, Bentham RB, Kotiadis VN, Menegollo M, Pignataro V, et al. Inositol trisphosphate receptor-mediated Ca²⁺ signalling stimulates mitochondrial function and gene expression in core myopathy patients. *Hum Mol Genet.* 2018; 27(13):2367-2382. doi: 10.1093/hmg/ddy149.
7. Brennan S, Garcia-Castañeda M, Michelucci A, Sabha N, Malik S, Groom L, et al. Mouse model of severe recessive RYR1-related myopathy. *Hum Mol Genet.* 2019; 28(18):3024-3036. doi: 10.1093/hmg/ddz105.
8. Capogrosso RF, Mantuano P, Uaesoontrachoon K, Cozzoli A, Giustino A, Dow T, et al. Ryanodine channel complex stabilizer compound S48168/ARM210 as a disease modifier in dystrophin-deficient mdx mice: proof-of-concept study and independent validation of efficacy. *FASEB J.* 2018; 32(2):1025-1043. doi: 10.1096/fj.201700182RRR.

9. Mori S, Inuma H, Manaka N, Ishigami-Yuasa M, Murayama T, Nishijima Y, et al. Structural development of a type-1 ryanodine receptor (RyR1) Ca-release channel inhibitor guided by endoplasmic reticulum Ca assay. *Eur J Med Chem.* 2019; 179:837-848. doi: 10.1016/j.ejmech.2019.06.076.
10. Zalk R, Clarke OB, des Georges A, Grassucci RA, Reiken S, Mancina F, et al. Structure of a mammalian ryanodine receptor. *Nature.* 2015; 517(7532):44-49. doi: 10.1038/nature13950.
11. Efremov RG, Leitner A, Aebersold R, Raunser S. Architecture and conformational switch mechanism of the ryanodine receptor. *Nature.* 2015; 517(7532):39-43. doi: 10.1038/nature13916.
12. Yan Z, Bai XC, Yan CY, Wu JP, Li ZQ, Xie T, et al. Structure of the rabbit ryanodine receptor RyR1 at near-atomic resolution. *Nature.* 2015; 517(7532):50-55. doi: 10.1038/nature14063.
13. Nasipak BT, Padilla-Benavides T, Green KM, Leszyk JD, Mao W, Konda S, et al. Opposing calcium-dependent signalling pathways control skeletal muscle differentiation by regulating a chromatin remodelling enzyme. *Nat Commun.* 2015; 6:7441. doi: 10.1038/ncomms8441.
14. Pisaniello A, Serra C, Rossi D, Vivarelli E, Sorrentino V, Molinaro M, et al. The block of ryanodine receptors selectively inhibits fetal myoblast differentiation. *J Cell Sci.* 2003; 116(Pt 8):1589-1597. doi: 10.1242/jcs.00358.
15. Bellinger AM, Reiken S, Dura M, Murphy PW, Deng SX, Landry DW, et al. Remodeling of ryanodine receptor complex causes "leaky" channels: a molecular mechanism for decreased exercise capacity. *Proc Natl Acad Sci U S A.* 2008; 105(6):2198-2202. doi: 10.1073/pnas.0711074105.
16. Fujii J, Otsu K, Zorzato F, de Leon S, Khanna VK, Weiler JE, et al. Identification of a mutation in porcine ryanodine receptor associated with malignant hyperthermia. *Science.* 1991; 253(5018):448-451. doi: 10.1126/science.1862346.
17. Filipova D, Walter AM, Gaspar JA, Brunn A, Linde NF, Ardestani MA, et al. Gene profiling of embryonic skeletal muscle lacking type I ryanodine receptor Ca(2+) release channel. *Sci Rep.* 2016; 6(1):20050. doi: 10.1038/srep20050.
18. Filipova D, Henry M, Rotshteyn T, Brunn A, Carstov M, Deckert M, et al. Distinct transcriptomic changes in E14.5 mouse skeletal muscle lacking RYR1 or Cav1.1 converge at E18.5. *PLoS ONE.* 2018; 13(3):e0194428. doi: 10.1371/journal.pone.0194428.
19. Ozcan L, Tabas I. Role of endoplasmic reticulum stress in metabolic disease and other disorders. *Annu Rev Med.* 2012; 63(63):317-328. doi: 10.1146/annurev-med-043010-144749.
20. Ron D, Walter P. Signal integration in the endoplasmic reticulum unfolded protein response. *Nat Rev Mol Cell Biol.* 2007; 8(7):519-529. doi: 10.1038/nrm2199.
21. Ozcan U, Cao Q, Yilmaz E, Lee AH, Iwakoshi NN, Ozdelen E, et al. Endoplasmic reticulum stress links obesity, insulin action, and type 2 diabetes. *Science.* 2004; 306(5695):457-461. doi: 10.1126/science.1103160.
22. Villalobos-Labra R, Subiabre M, Toledo F, Pardo F, Sobrevia L. Endoplasmic reticulum stress and development of insulin resistance in adipose, skeletal, liver, and foetoplacental tissue in diabetes. *Mol Aspects Med.* 2019; 66:49-61. doi: 10.1016/j.mam.2018.11.001.

23. Jheng JR, Chen YS, Ao UI, Chan DC, Huang JW, Hung KY, et al. The double-edged sword of endoplasmic reticulum stress in uremic sarcopenia through myogenesis perturbation. *J Cachexia Sarcopenia Muscle*. 2018; 9(3):570-584. doi: 10.1002/jcsm.12288.
24. Bohnert KR, McMillan JD, Kumar A. Emerging roles of ER stress and unfolded protein response pathways in skeletal muscle health and disease. *J Cell Physiol*. 2018; 233(1):67-78. doi: 10.1002/jcp.25852.
25. Nakanishi K, Dohmae N, Morishima N. Endoplasmic reticulum stress increases myofiber formation in vitro. *FASEB J*. 2007; 21(11):2994-3003. doi: 10.1096/fj.06-6408com.
26. Nakanishi K, Sudo T, Morishima N. Endoplasmic reticulum stress signaling transmitted by ATF6 mediates apoptosis during muscle development. *J Cell Biol*. 2005; 169(4):555-560. doi: 10.1083/jcb.200412024.
27. Günther S, Kim J, Kostin S, Lepper C, Fan CM, Braun T. Myf5-Positive Satellite Cells Contribute to Pax7-Dependent Long-Term Maintenance of Adult Muscle Stem Cells. *Cell Stem Cell*. 2013; 13(5):590-601. doi: 10.1016/j.stem.2013.07.016.
28. Qiu K, Xu D, Wang L, Zhang X, Jiao N, Gong L, et al. Association Analysis of Single-Cell RNA Sequencing and Proteomics Reveals a Vital Role of Ca Signaling in the Determination of Skeletal Muscle Development Potential. *Cells*. 2020; 9(4): 1045. doi: 10.3390/cells9041045.
29. Ikemoto T, Hosoya T, Aoyama H, Kihara Y, Suzuki M, Endo M. Effects of dantrolene and its derivatives on Ca²⁺ release from the sarcoplasmic reticulum of mouse skeletal muscle fibres. *Br J Pharmacol*. 2010; 134(4):729-736. doi: 10.1038/sj.bjp.0704307.
30. Comai G, Tajbakhsh S. Molecular and Cellular Regulation of Skeletal Myogenesis. *Curr Top Dev Biol*. 2014; 110:1-73. doi: 10.1016/B978-0-12-405943-6.00001-4.
31. Bijlenga P, Liu JH, Espinos E, Haenggeli CA, Fischer-Lougheed J, Bader CR, et al. T-Type α 1H Ca²⁺Channels Are Involved in Ca²⁺Signaling during Terminal Differentiation (Fusion) of Human Myoblasts. *Proc Natl Acad Sci U S A*. 2000; 97(13):7627-7632. doi: 10.1073/pnas.97.13.7627.
32. Porter Jr GA, Makuck RF, Rivkees SA. Reduction in intracellular calcium levels inhibits myoblast differentiation. *J Biol Chem*. 2002; 277(32):28942-28947. doi: 10.1074/jbc.M203961200.
33. Qiu K, Zhang X, Wang L, Jiao N, Xu D, Yin J. Protein expression landscape defines the differentiation potential specificity of adipogenic and myogenic precursors in the skeletal muscle. *J Proteome Res*. 2018; 17(11):3853-3865. doi: 10.1021/acs.jproteome.8b00530.
34. Airey JA, Baring MD, Sutko JL. Ryanodine receptor protein is expressed during differentiation in the muscle cell lines BC3H1 and C2C12. *Dev Biol*. 1991; 148(1):365-374. doi: 10.1016/0012-1606(91)90344-3.
35. Raffaello A, Mammucari C, Gherardi G, Rizzuto R. Calcium at the Center of Cell Signaling: Interplay between Endoplasmic Reticulum, Mitochondria, and Lysosomes. *Trends Biochem Sci*. 2016; 41(12):1035-1049. doi: 10.1016/j.tibs.2016.09.001.
36. Rink TJ. Receptor-mediated calcium entry. *Febs Letters*. 1990; 268(2):381-385.

37. Mackrill JJ. Protein–protein interactions in intracellular Ca²⁺-release channel function. *Biochem J.* 1999; 337 (Pt 3)(3):345-361.
38. Villalobos C, García-sancho J. Capacitative Ca²⁺ entry contributes to the Ca²⁺ influx induced by thyrotropin-releasing hormone (TRH) in GH3 pituitary cells. *Pflügers Arch.* 1995; 430(6):923-935. doi: 10.1007/BF01837406.
39. Misquitta CM, Mack DP, Grover AK. Sarco/endoplasmic reticulum Ca²⁺ (SERCA)-pumps: link to heart beats and calcium waves. *Cell Calcium.* 1999; 25(4):277-290. doi: 10.1054/ceca.1999.0032.
40. Bruce JIE. Metabolic regulation of the PMCA: Role in cell death and survival. *Cell Calcium.* 2018; 69:28-36. doi: 10.1016/j.ceca.2017.06.001.
41. Brini M, Carafoli E. The Plasma Membrane Ca²⁺ ATPase and the Plasma Membrane Sodium Calcium Exchanger Cooperate in the Regulation of Cell Calcium. *Cold Spring Harb Perspect Biol.* 2011; 3(2):487-496. doi: 10.1101/cshperspect.a004168.
42. Shaw PJ, Qu B, Hoth M, Feske S. Molecular regulation of CRAC channels and their role in lymphocyte function. *Cell Mol Life Sci.* 2013; 70(15):2637-2656. doi: 10.1007/s00018-012-1175-2.
43. Prakriya, Murali. Store-operated calcium channels: Academic Press; 2013.757-810.
44. Tapscott SJ. The circuitry of a master switch: MyoD and the regulation of skeletal muscle gene transcription. *Development.* 2005; 132(12):2685-2695. doi: 10.1242/dev.01874.
45. Saab R, Spunt SL, Skapek SX. Myogenesis and Rhabdomyosarcoma : The Jekyll and Hyde of Skeletal Muscle. *Curr Top Dev Biol.* 2011; 94(94):197-234. doi: 10.1016/B978-0-12-380916-2.00007-3.
46. Schartner V, Romero NB, Donkervoort S, Treves S, Munot P, Pierson TM, et al. Dihydropyridine receptor (DHPR, CACNA1S) congenital myopathy. *Acta neuropathol.* 2017; 133(4):517-533. doi: 10.1007/s00401-016-1656-8.
47. Anelli T, Alessio M, Bachi A, Bergamelli L, Bertoli G, Camerini S, et al. Thiol-mediated protein retention in the endoplasmic reticulum: the role of ERp44. *EMBO J.* 2003; 22(19):5015-5022. doi: 10.1093/emboj/cdg491.
48. Hetz C. The unfolded protein response: controlling cell fate decisions under ER stress and beyond. *Nat Rev Mol Cell Biol.* 2012; 13(2):89-102. doi: 10.1038/nrm3270.
49. Urano F, Wang X, Bertolotti A, Zhang Y, Chung P, Harding HP, et al. Coupling of stress in the ER to activation of JNK protein kinases by transmembrane protein kinase IRE1. *Science.* 2000; 287(5453):664-666. doi: 10.1126/science.287.5453.664.
50. Chen Q, Hang Y, Zhang T, Tan L, Li S, Jin Y. USP10 promotes proliferation and migration and inhibits apoptosis of endometrial stromal cells in endometriosis through activating the Raf-1/MEK/ERK pathway. *Am J Physiol Cell Physiol.* 2018; 315(6):C863-C872. doi: 10.1152/ajpcell.00272.2018.
51. Abdullahi A, Stanojcic M, Parousis A, Patsouris D, Jeschke MG. Modeling Acute ER Stress in Vivo and in Vitro. *Shock.* 2017; 47(4):506-513. doi: 10.1097/SHK.0000000000000759.

52. Földi I, Tóth AM, Szabó Z, Mózes E, Berkecz R, Datki ZL, et al. Proteome-wide study of endoplasmic reticulum stress induced by thapsigargin in N2a neuroblastoma cells. *Neurochem Int.* 2013; 62(1):58-69. doi: 10.1016/j.neuint.2012.11.003.
53. Zhang X, Yuan Y, Jiang L, Zhang J, Gao J, Shen Z, et al. Endoplasmic reticulum stress induced by tunicamycin and thapsigargin protects against transient ischemic brain injury: Involvement of PARK2-dependent mitophagy. *Autophagy.* 2014; 10(10):1801-1813. doi: 10.4161/auto.32136.
54. Wang Y, Zhu J, Zhang L, Zhang Z, He L, Mou Y, et al. Role of C/EBP homologous protein (CHOP) and Endoplasmic Reticulum in Asthma Exacerbation by Regulating the IL-4/STAT6/Tfec/IL-4R α Positive Feedback Loop in M2 Macrophages. *J Allergy Clin Immunol.* 2017; 140(6):1550-1561. doi: 10.1016/j.jaci.2017.01.024.
55. Hermel E, Klapstein KD. A possible mechanism for maintenance of the deleterious allele of human CASPASE-12. *Med Hypotheses.* 2011; 77(5):803-806. doi: 10.1016/j.mehy.2011.07.041.
56. Nakagawa T, Zhu H, Morishima N, Li E, Xu J, Yankner BA, et al. Caspase-12 mediates endoplasmic-reticulum-specific apoptosis and cytotoxicity by amyloid-beta. *Nature.* 2000; 403(6765):98-103. doi: 10.1038/47513.
57. Westphal D, Kluck RM, Dewson G. Building blocks of the apoptotic pore: how Bax and Bak are activated and oligomerize during apoptosis. *Cell Death Differ.* 2014; 21(2):196-205. doi: 10.1038/cdd.2013.139.
58. Wang J, Lee J, Liem D, Ping P. HSPA5 Gene encoding Hsp70 chaperone BiP in the endoplasmic reticulum. *Gene.* 2017; 618:14-23. doi: 10.1016/j.gene.2017.03.005.
59. Bakunts A, Orsi A, Vitale M, Cattaneo A, Lari F, Tadè L, et al. Ratiometric sensing of BiP-client versus BiP levels by the unfolded protein response determines its signaling amplitude. *eLife.* 2017; 6:e27518. doi: 10.7554/eLife.27518.
60. Rosenbaum M, Andreani V, Kapoor T, Herp S, Flach H, Duchniewicz M, et al. MZB1 is a GRP94 cochaperone that enables proper immunoglobulin heavy chain biosynthesis upon ER stress. *Genes Dev.* 2014; 28(11):1165-1178. doi: 10.1101/gad.240762.114.
61. Anelli T, Alessio M, Mezghrani A, Simmen T, Talamo F, Bachi A, et al. ERp44, a novel endoplasmic reticulum folding assistant of the thioredoxin family. *EMBO J.* 2002; 21(4):835-844. doi: 10.1093/emboj/21.4.835.
62. Yang Z, Zhuang L, Szatmary P, Wen L, Sun H, Lu Y, et al. Upregulation of heat shock proteins (HSPA12A, HSP90B1, HSPA4, HSPA5 and HSPA6) in tumour tissues is associated with poor outcomes from HBV-related early-stage hepatocellular carcinoma. *Int J Med Sci.* 2015; 12(3):256-263. doi: 10.7150/ijms.10735.
63. Brillantes AB, Ondrias K, Scott A, Kobrinsky E, Ondriasová E, Moschella MC, et al. Stabilization of calcium release channel (ryanodine receptor) function by FK506-binding protein. *Cell.* 1994; 77(4):513-523. doi: 10.1016/0092-8674(94)90214-3.
64. Marx SO, Reiken S, Hisamatsu Y, Gaburjakova M, Gaburjakova J, Yang YM, et al. Phosphorylation-dependent regulation of ryanodine receptors: a novel role for leucine/isoleucine zippers. *J Cell Biol.*

- 2001; 153(4):699-708. doi: 10.1083/jcb.153.4.699.
65. Guerrero-Hernández A, Ávila G, Rueda A. Ryanodine receptors as leak channels. *Eur J Pharmacol.* 2014; 739:26-38. doi: 10.1016/j.ejphar.2013.11.016.
66. Thrivikraman G, Madras G, Basu B. Electrically driven intracellular and extracellular nanomanipulators evoke neurogenic/cardiomyogenic differentiation in human mesenchymal stem cells. *Biomaterials.* 2016; 77:26-43. doi: 10.1016/j.biomaterials.2015.10.078.
67. Feng R, Zhai WL, Yang HY, Jin H, Zhang QX. Induction of ER stress protects gastric cancer cells against apoptosis induced by cisplatin and doxorubicin through activation of p38 MAPK. *Biochem Biophys Res Commun.* 2011; 406(2):299-304. doi: 10.1016/j.bbrc.2011.02.036.
68. Wang H, Dong Y, Zhang J, Xu Z, Wang G, Swain CA, et al. Isoflurane induces endoplasmic reticulum stress and caspase activation through ryanodine receptors. *Br J Anaesth.* 2014; 113(4):695-707. doi: 10.1093/bja/aeu053.

Figures

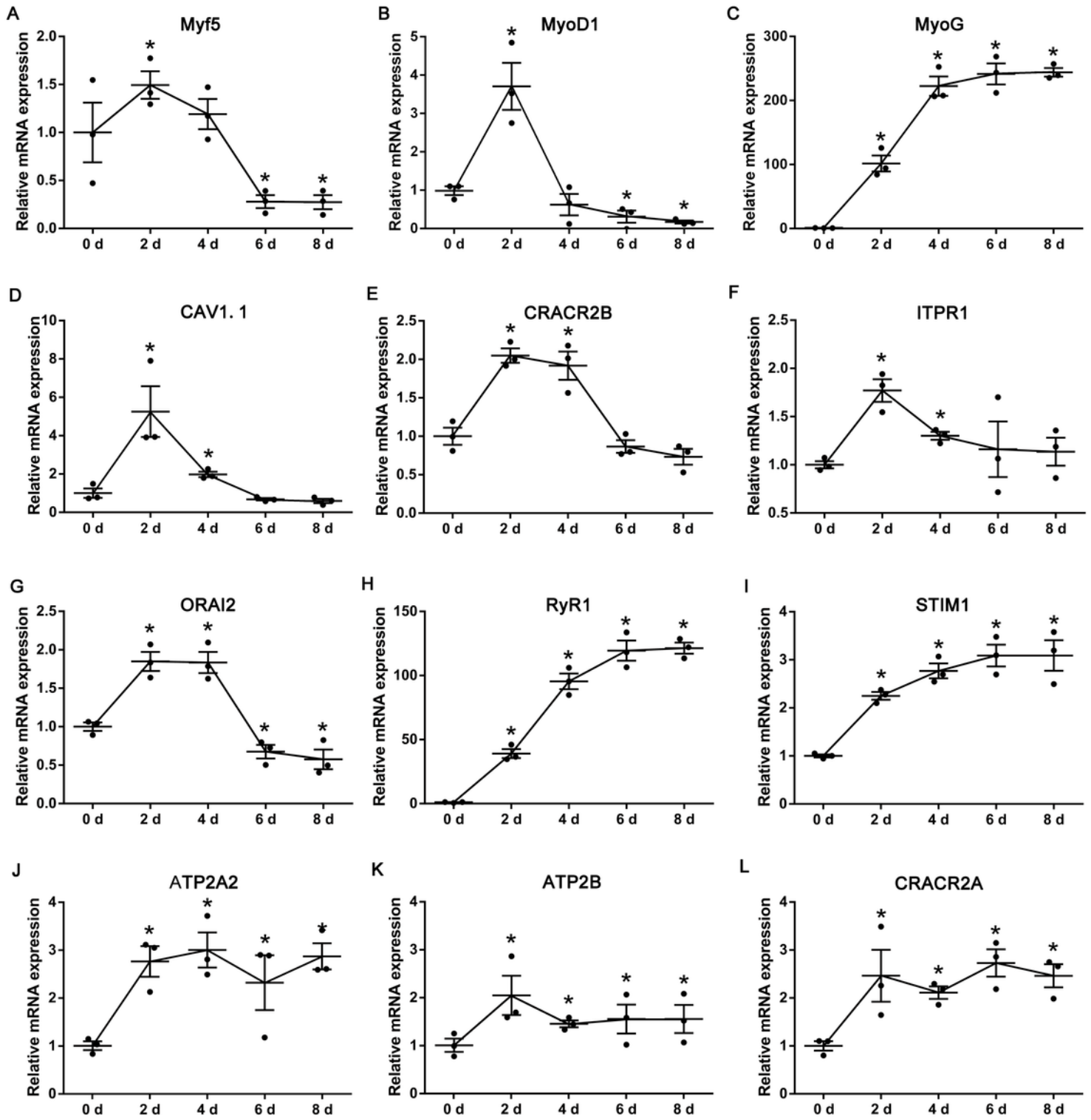


Figure 1

Relative mRNA expression of Myf5 (A), MyoD1 (B), MyoG (C), CAV1.1 (D), CRACR2B (E), ITPR1 (F), ORAI2 (G), RyR1 (H), STIM1 (I) ATP2A2 (J), ATP2B (K), and CRACR2A (L), on day 0, 2, 4, 6, and 8 during myogenic differentiation of C2C12 cells (n = 3). The data are presented as the mean ± SEM. *Represents significant difference with the value on day 0 (P < 0.05).

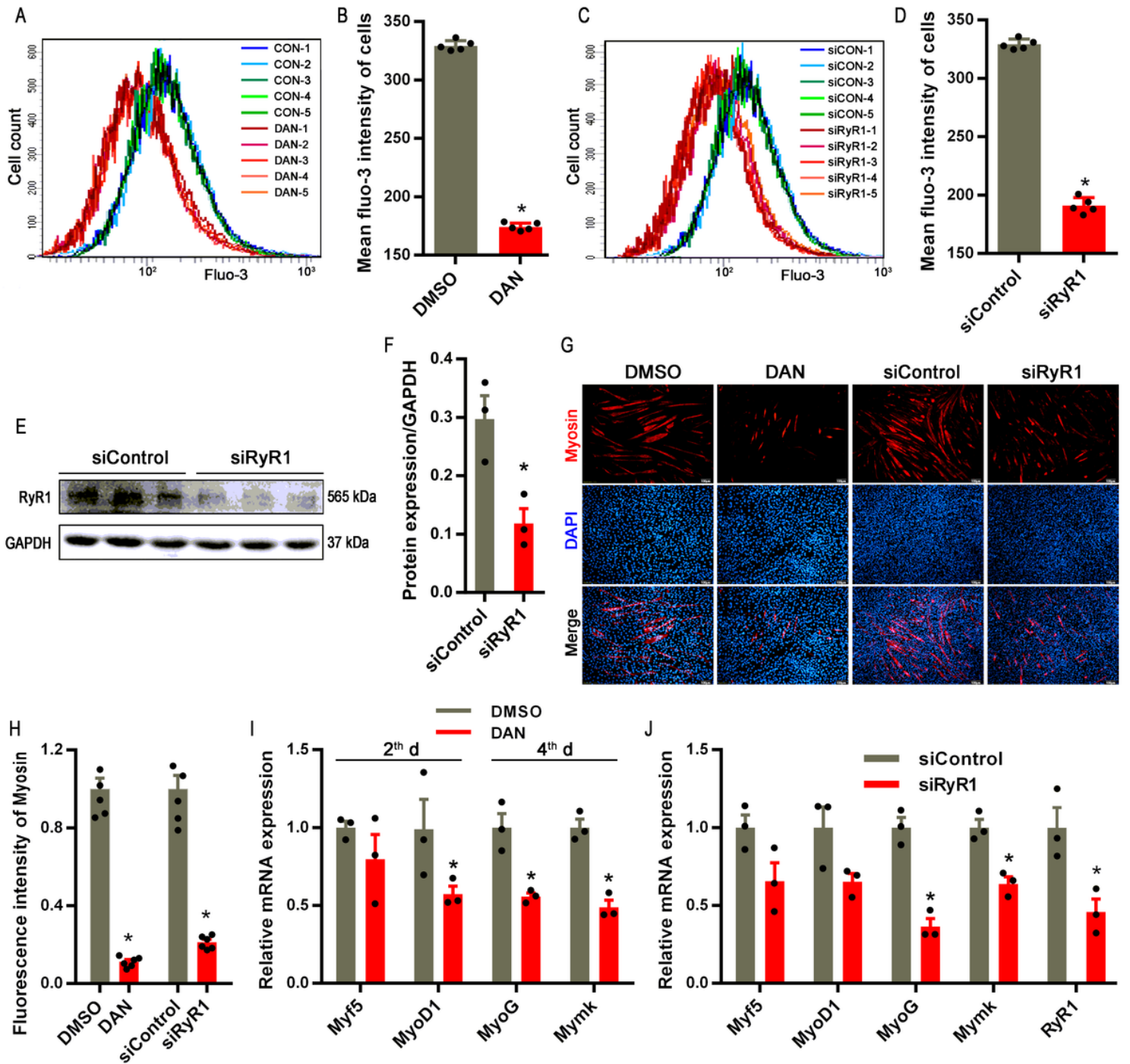


Figure 2

The effects of RyR1 restriction on myogenic differentiation of C2C12 myoblasts. (A-B) The concentration of cytoplasmic Ca²⁺ labeled by Fluo-3 treated with Dantrolene (DAN, 10 μ M, RyR1 inhibitor) for 48 h (n = 5). (C-D) The concentration of cytoplasmic Ca²⁺ labeled by Fluo-3 in C2C12 cells transfected with siRyR1 for 72 h (n = 5). (E-F) The proteins expression of RyR1 in C2C12 cells after myogenic induction for 5 days with siRyR1 transfection (n = 3). (G) Immunostaining with myosin antibody of C2C12 cells after myogenic induction for 5 days with DAN treatment or siRyR1 transfection. (H) Fluorescence intensity of myosin in G (n = 6). (I) Relative mRNA expression of related genes in C2C12 cells treated with DAN on day

2 (Myf5 and MyoD1) and 4 (MyoG and Mymk) of myogenic differentiation (n = 3). (J) Relative mRNA expression of RyR1, Myf5, MyoD1, MyoG, and Mymk in C2C12 cells transfected with siRyR1 for 72 h (n = 3). *Represents significant difference between the two groups (P < 0.05).

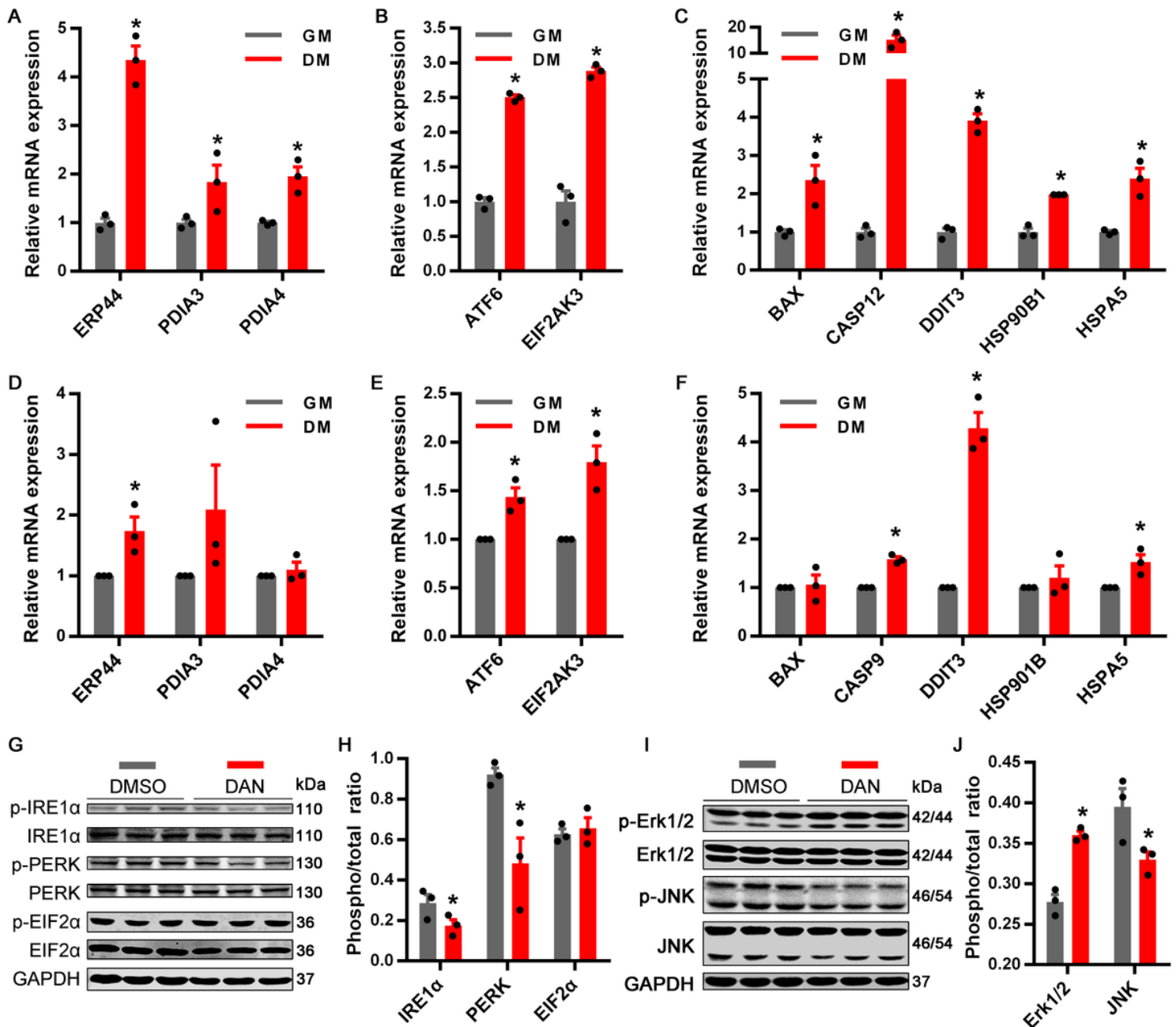


Figure 3

Endoplasmic reticulum (ER) stress of myoblasts during proliferation and myogenic differentiation (n = 3). (A-C) Relative mRNA expression of genes related ER stress, unfolded protein response, and apoptosis respectively in C2C12 cells. (D-F) Relative mRNA expression of genes related ER stress, unfolded protein response, and apoptosis respectively in skeletal muscle derived myoblasts of pigs. (G-J) The expression of proteins related to ER stress and MAPK signaling in C2C12 cells during proliferation treated with Dantrolene (DAN, 10 μM, RyR1 inhibitor) for 48 h (n = 5). GM, growth medium, representing cells cultured in growth medium before myogenic induction; DM, differentiation medium, representing cells on day 4

during myogenic differentiation cultured in differentiation medium. The data are presented as the mean \pm SEM. *Represents significant difference between the two groups ($P < 0.05$).

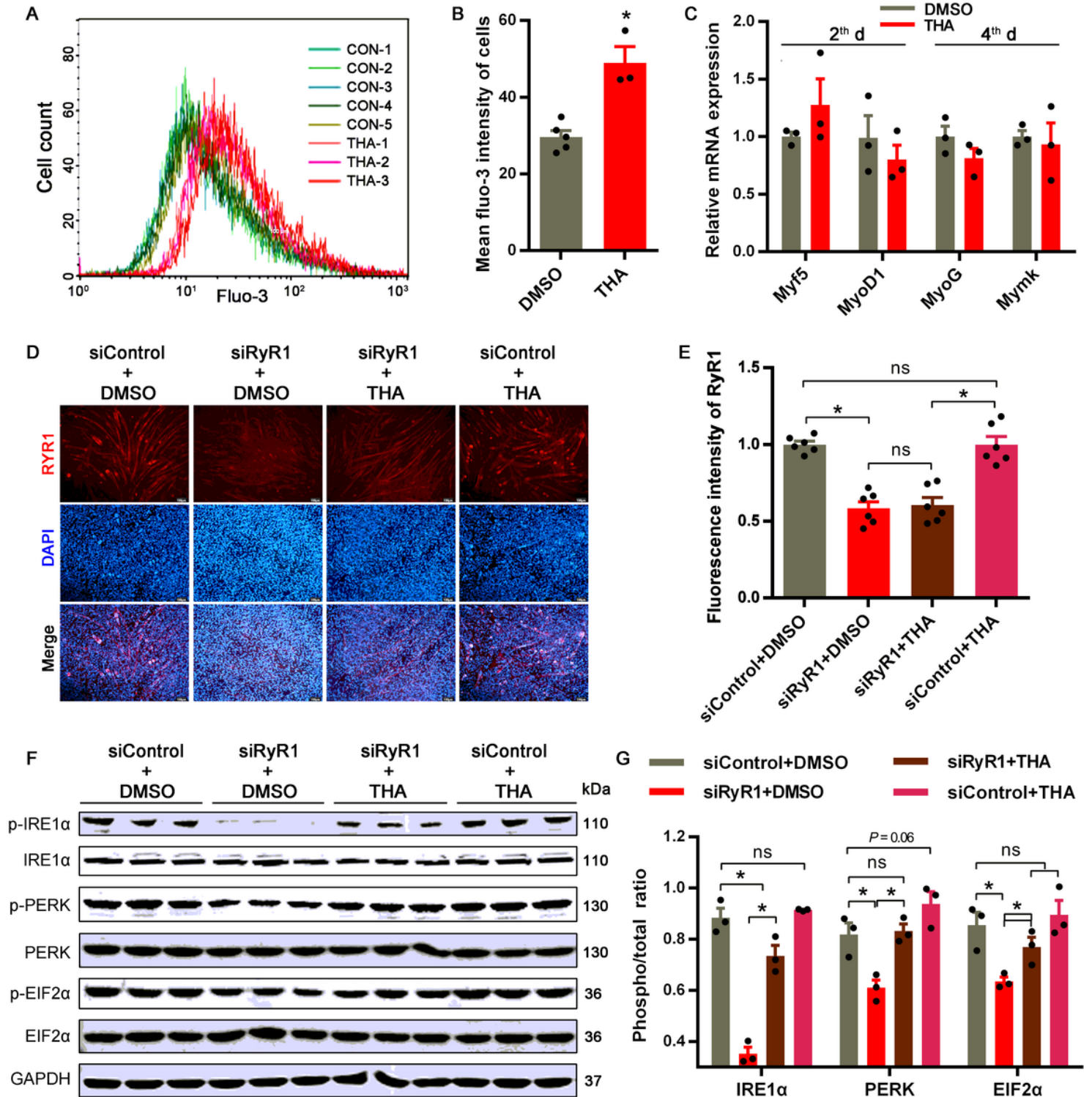


Figure 4

Controlling of RyR1-mediated endoplasmic reticulum stress. (A-B) The concentration of cytoplasmic Ca²⁺ labeled by Fluo-3 in C2C12 cells treated with Thapsigargin (THA) for 48 h (n = 3). (C) Relative mRNA expression of related genes in C2C12 cells treated with THA on day 2 (Myf5 and MyoD1) and 4

(MyoG and Mymk) during myogenic differentiation (n = 3). (D) Immunostaining with RyR1 antibody of C2C12 cells after myogenic induction for 5 days treated with siRyR1 or THA. (E) Fluorescence intensity of RyR1 (n = 5). (F-G) The expression of proteins related to ER stress in C2C12 cells after myogenic induction for 5 days treated with siRyR1 or THA (n = 3). The data are presented as the mean \pm SEM. *Represents significant difference between the two groups (P < 0.05).

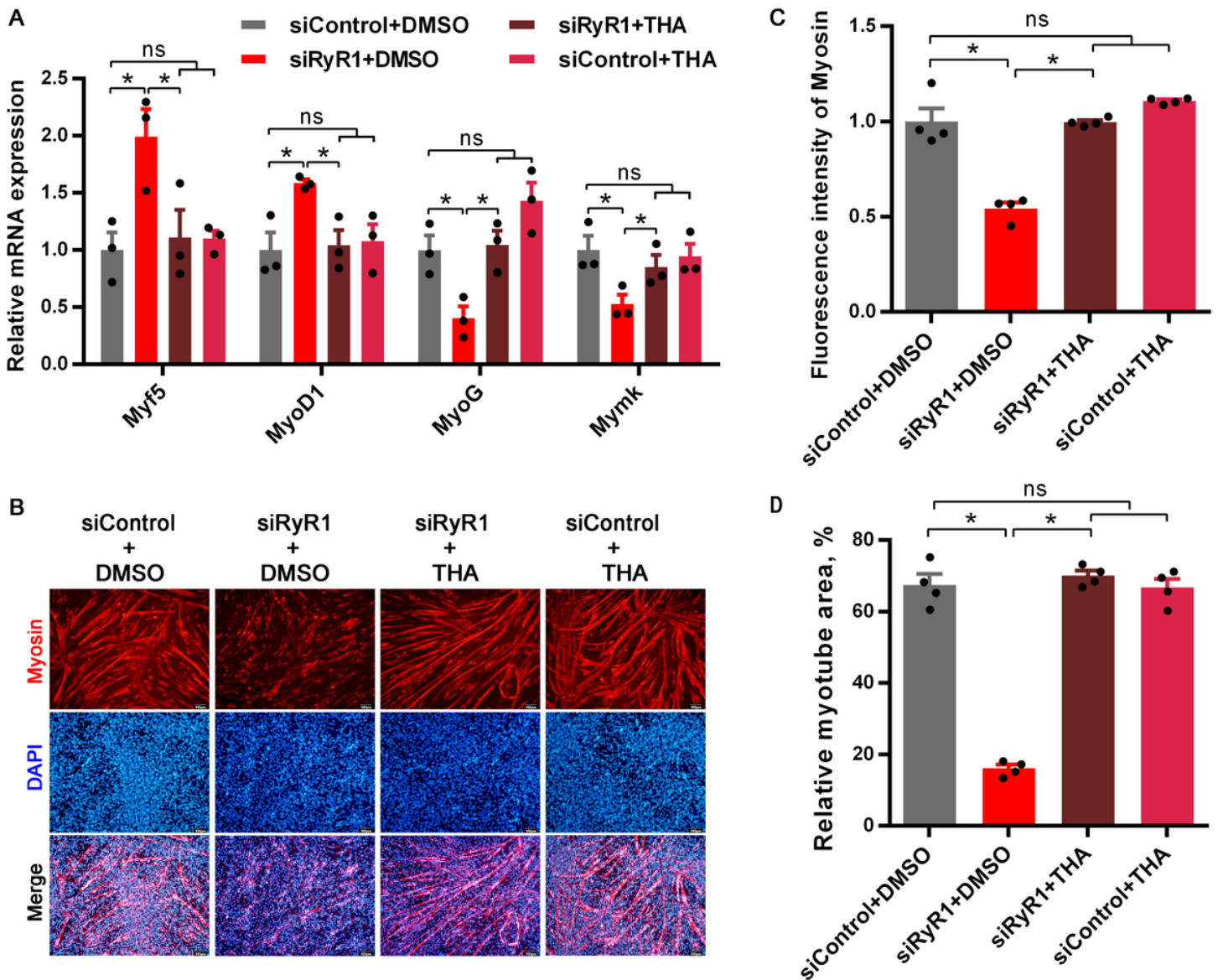


Figure 5

Activation of endoplasmic reticulum stress signaling was indispensable in RyR1-mediated myogenic differentiation of C2C12 myoblasts. (A) Relative mRNA expression of Myf5, MyoD1, MyoG, and Mymk after the treatments with siRyR1 or Thapsigargin (THA) after myogenic induction for 4 days (n = 3). (B) Immunostaining with myosin antibody after myogenic induction for 5 days treated with siRyR1 or THA. (C) Fluorescence intensity of myosin (n = 4). (D) The relative myotube area. The data are presented as the mean \pm SEM. *Represents significant difference between the two groups (P < 0.05).

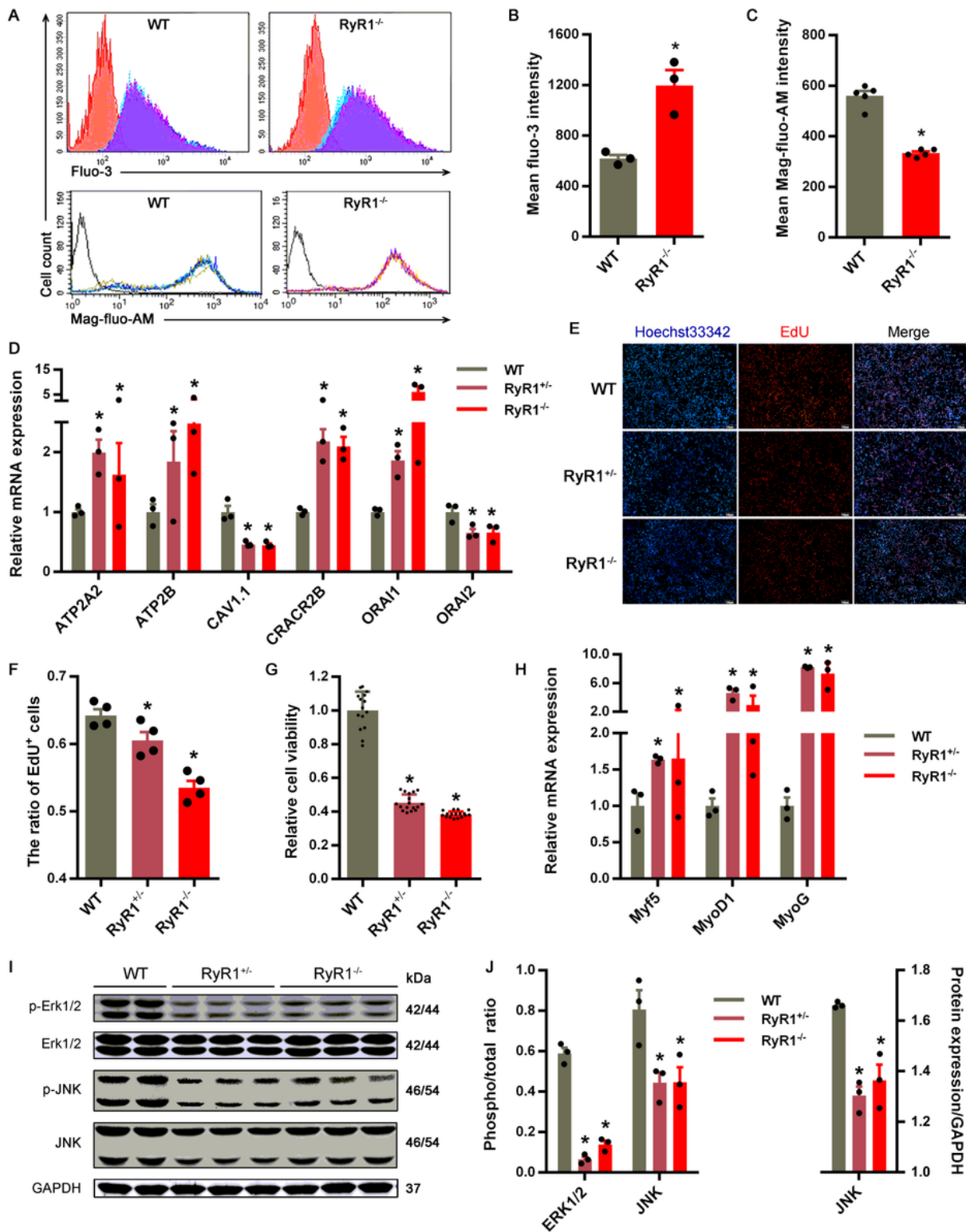


Figure 6

The effects of RyR1-knockout on cellular Ca²⁺ dynamics and differentiation of C2C12 myoblasts. (A-C) The concentration of Ca²⁺ in cytoplasm (labeled by Fluo-3, n = 3) and endoplasmic reticulum (labeled by Fluo-4, n = 5) of RyR1-KO cells. (D) The effect of RyR1-KO on the mRNA expression of Ca²⁺ channels (n = 3). (E-G) Proliferation and viability of RyR1-KO cells measured by EdU staining or CCK-8 test (n = 10). (H) Relative mRNA expression of Myf5, MyoD1, and MyoG in RyR1-KO cells (n = 3). (I-J) The expression of

proteins related to MAPK signaling in RyR1-KO cells (n = 3). RyR1^{-/-} and RyR1^{+/-} represent homozygote and heterozygote of RyR1-knockout respectively. The data are presented as the mean ± SEM. *Represents significant difference between the two groups (P < 0.05).

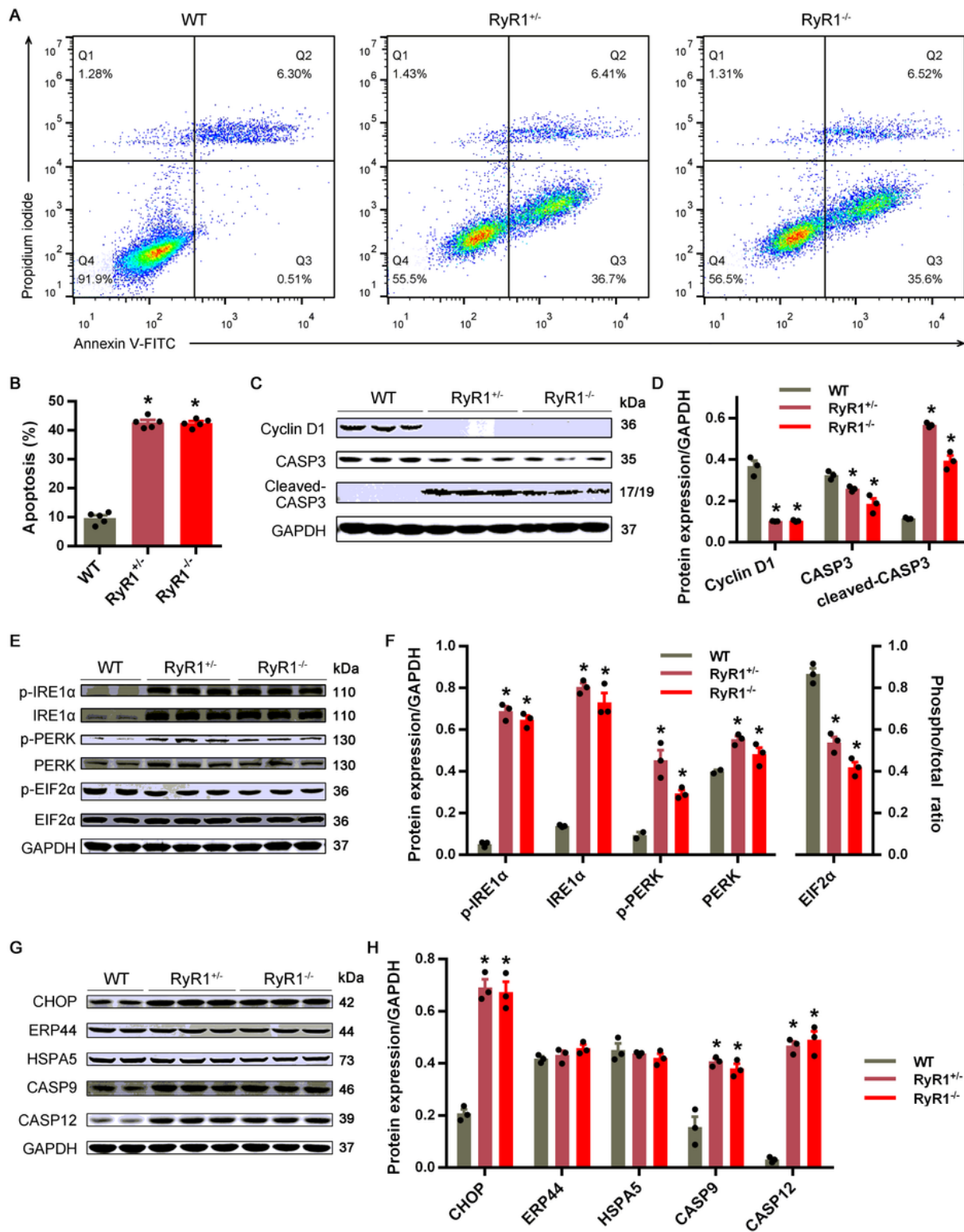


Figure 7

Endoplasmic reticulum stress-associated apoptosis in C2C12 cells was induced by RyR1-knockout (n = 3). (A-B) Apoptosis detection of RyR1-null cells through flow cytometry. (C-D) The protein expression of

Cyclin D1, caspase-3 (CASP3), and cleaved-CASP3 in RyR1-KO cells. (E-H) The expression of proteins related to ER stress or ER stress-induced apoptosis in RyR1-KO cells. RyR1^{-/-} and RyR1^{+/-} represent homozygote and heterozygote of RyR1-knockout, respectively. The data are presented as the mean \pm SEM. *Represents significant difference between the two groups ($P < 0.05$).

Supplementary Files

This is a list of supplementary files associated with this preprint. Click to download.

- [FigureS1.tif](#)
- [FigureS2.tif](#)
- [FigureS3.tif](#)
- [TableS1.pdf](#)
- [TableS2.pdf](#)
- [TableS3.pdf](#)
- [TableS4.pdf](#)